Title	Effect of swirl on the interaction between laterally placed tidal turbines using actuator-disc based numerical simulations
Authors	Rafa Baptista Ochoa, Vikrant Gupta and Anna Mollie Young
Number (ENG-TR)	ENG-TR.002
Date	13 May 2020
ISSN	2633-6839

Effect of swirl on the interaction between laterally placed tidal turbines using actuator-disc based numerical simulations

Rafa Baptista Ochoa, Vikrant Gupta, Anna Mollie Young

Much of the future potential for tidal energy lies in tidal channels, where turbines can be arranged in an array in such a way as to exploit the effects of channel blockage and thus increase performance. One such strategy employed by researchers has been to have an array of turbines which only partially blocks the channel width. Previous work, employing mass and momentum conservation and considering the turbines as simple actuator disks, has shown that the local arrangement of the turbines can be altered in a way that optimises the power output of the whole array. However, real turbines also impart swirl to the flow. When this swirl imposed on the flow by the turbines is taken into account by modelling the turbines with Blade Element Momentum Theory (BEMT) discs, further interaction effects become apparent. These effects depend on the proximity of the turbines to one another and can have a significant impact on the optimal arrangement of the devices in a given channel. This report demonstrates the key effects by comparing sets of actuator disc simulations with and without BEMT, and makes the case for taking swirl effects into account when designing tidal arrays computationally. The other benefit of using BEMT discs is that they rely only on known, physical characteristics of the turbines (i.e. lift and drag performance curves) as opposed to estimated quantities (i.e. the momentum extraction coefficient). This means that real turbines can be simulated with more accuracy. It will be argued in this paper that these twin advantages of increased realism in both the flow field and the turbine outweigh the negligible increase in computing power required to undertake BEMT simulations and so these simulations should be the minimum standard for tidal array designs.

Keywords: Tidal energy, Tidal fence, Hydraulics, Actuator disc models

1 INTRODUCTION

Many recent plans for investment in tidal power in the UK are focused on the exploitation of tidal channels. Sites such as the Pentland Firth, near the Orkney Islands off the northern coast of Scotland, provide a significant potential for power extraction; this site alone could provide 1.8 GW [1].

The task of arranging turbines in these channels is a complex one. Placing too few turbines in each array means that the site is under-exploited, while adding too many devices to the array can choke the flow and limit the power output [2]. This suggests that there will be an optimal arrangement of turbines in a channel, given both in terms of the number of turbines in the array and their spacing across the channel. There have been several approaches to the problem of finding the optimal placement of tidal turbines in a channel. One of the earliest approaches was that of Garrett and Cummins [2], where they expressed the maximum available power potential of a tidal channel in terms of its tidal head. They obtained an analytical expression and showed that the available power is higher than the Betz limit [3], often used in wind power; this is due to the fact that the flow is constrained in a tidal channel. However, Garrett and Cummins [2] assumed a simplified setup where the position of the tidal array and the number and location of the devices are not considered. Bryden *et al.* [4] proposed an enhanced model where the effect of power extraction by upstream devices on those further downstream is considered, but the set up is still idealised.

Garrett and Cummins [5] modified their earlier model to allow for non-uniform flow profiles across channels, due to, for example, side corridors set aside for navigation, and proposed tuning the turbines to the flow so as to achieve an optimal flow velocity downstream. The optimal tuning of turbine arrays to velocity profiles was investigated further by Vennell [6, 7], again making use of a simplified 1D model.

The seminal paper in the analytical approach to the optimal design of tidal arrays in channels is that of Nishino and Willden [8], where the authors postulated a more comprehensive 2D setup, explicitly modelling the wake behind the devices. By making use of the 'two-scale assumption' that device scale disturbances in the flow are dissipated quickly compared to array-scale disturbances, they obtained an expression for the power potential of a channel with respect to the number of devices in the array, hence finding the optimal number of turbines. They also backed up their analytical results using actuator disc CFD simulations, described later in this section.

Another strand of the literature has used a more detailed numerical approach, based on the shallow water equations and using real bathymetry data for sites of interest. A study by Adcock *et al.* [9] used detailed data for the Pentland Firth. By meshing the whole channel and choosing the most likely locations for turbine arrays, they solved the shallow water equations for several different scenarios and obtained realistic estimates of the power potential of the site. Their approach, however, shows why a detailed CFD simulation of tidal channels is impractical: the length-scales for which the flow must be solved range from the blade boundary layer (centimetres) to the channel width (kilometres), and therefore the simulations are not feasible with today's computing power (especially not for an industrial turbine developer).

One compromise between the simplified, analytical approach, and the detailed CFD simulation is to represent the turbines as actuator discs. The actuator disc model was first

used for modelling helicopter rotors [10] and ship propellers [11]. After being adapted for wind energy [12], the method was soon applied to modelling tidal farms (for some examples, see [13, 14]). The method involves in solving the Reynolds- averaged Navier Stokes (RANS) equations in a CFD simulation where the turbine is replaced by a thin, disc-shaped region which removes axial momentum from the surrounding flow to represent both the useful power generated by the turbine and the losses. Batten and Bahaj [15] have made use of this method to estimate the power potential of tidal sites. The study by Nishino and Willden [8] mentioned above also used actuator disc CFD simulations to validate their analytical findings.

A key shortcoming of the actuator disc approach is that it does not model the swirl induced by the turbines on the flow, and hence relies on the assumption that the changes in tangential velocity are only important in the vicinity of the devices, and can be safely neglected further downstream. This assumption can be dropped by using Blade Element Momentum Theory (BEMT), which enables swirl effects to be included at the device scale. This modelling approach is also known as a RANS + BE disc, where RANS stands for Reynolds-averaged Navier-Stokes. The two approaches (which will be referred to in this paper as the 'simple' disc and the BEMT disc) have been compared by Batten *et al.* [16] by replicating an experimental setup using a towing tank and a single turbine. As expected, the BEMT disc gave better agreement with the experiments than the simple disc.

To the authors' knowledge, there have so far been no simulations of tidal arrays using BEMT discs. The work presented in this report shows that simulating an array using BEMT discs gives a flow field which is both quantitatively and qualitatively different from the solution generated using simple discs. The differences arise due to the introduction of swirl by the BEMT discs leading to highly distorted wakes, longer dissipation lengths, and regions of flow recirculation (negative axial velocity). Quantitatively, there are significant changes in the power coefficients of the discs when compared with simple disc simulations. In addition, all the effects of swirl are highly dependent on the proximity of the turbines to one another.

This study considers simulations of arrays of 5 turbines inside rectangular channels with two different levels of global blockages. First, a qualitative comparison of simple actuator disc simulations (with no swirl) and BEMT-enhanced discs (with swirl) is presented. Then, a quantitative comparison of power coefficients against disc spacing is given for both types of simulation.

2 METHOD

A series of RANS simulations were undertaken of a turbine array inside a rectangular channel, in which the turbines were represented as actuator discs. The devices were replaced by thin, disc-shaped cell zones within which a series of source terms are applied. Two different types of actuator disc were considered: 'simple' discs, which included only an axial momentum sink, and Blade Element Momentum Theory (BEMT) discs, which included source terms in the tangential as well as the axial direction. For simplicity, the two models are referred to as 'simple discs' and 'BEMT discs' respectively. It should be noted that the source terms in BEMT discs come from the blade's lift and drag coefficients (C_L and C_D) and vary radially. In contrast to that, the source term in simple discs come from the drag imposed by the turbine

on the flow and is radially constant. This enables BEMT discs to represent the turbines much more faithfully than is possible for simple discs at no added computational cost, except for the predetermination of C_L and C_D coefficients as explained in Section 2.3.

For the purpose of obtaining a normalising benchmark, a single device was modelled for each type of disc and for each channel blockage; this case is described first. Then, the full array case containing 5 devices is described.

2.1 Geometry and mesh

The benchmark case consists of a single disc centred inside a rectangular channel. A schematic of the domain is given in Figure 2.1. The turbine modelled has a diameter of 18 m, and the thickness of the disc is fixed to 1/100 of the diameter (as recommended by Batten *et al.* [16]). The meshing was carried out using ANSYS ICEM. In addition, for BEMT discs, it is common practice to include the effect of the nacelle in the centre of the disc, which is modelled as a smaller solid disc with no flow at the centre of the actuator disc, with the same thickness as the actuator disc and a diameter representative of a real turbine (in this case, 1.75 m).

The full tidal array case simulated in this study consists of five discs, each of the same dimensions and aligned in the axial direction. The array is centred inside a rectangular channel and the turbines are spaced uniformly with gaps which were varied between 0.25 and 3 diameters. A schematic of the domain is given in Figure 2.2(a). The labelling of the discs within the array is also shown in Figure 2.2(b). The full array channels had the same depth as the benchmark, single disc cases, but the width of the channel was modified in order to achieve the same level of global blockage in each case.

For the simple disc cases, the geometry has two planes of symmetry, and hence only one quarter of the channel needs to be meshed (the free surface is not being modelled - see below). For BEMT discs, because the source terms applied within the disc introduce tangential velocity, the problem no longer has any planes of symmetry and hence the whole channel must be meshed. This is shown in Figure 2.3.

Finally, it should be noted that since the outflow boundary condition imposes zero gradient on some properties, the mesh must be allowed to extend far enough downstream of the turbines in order not to disturb the wakes. For this reason, the length of the channel was set to 30 diameters for the single-disc benchmark case, and to 70 diameters for the full array case.

2.2 CFD solver

The solver used in the project is ANSYS Fluent, a pressure-based RANS flow solver which has been used extensively for incompressible flow in both academia and industry.

The boundary condition at all the side walls was set to no-shear, because the effect of the proximity of side walls was not being considered in this study. The same no-shear condition was also applied to the sea surface and the seabed. The boundary condition for the seabed could have been set to no-slip to take seabed friction into account. Seabed friction has been shown to have a major impact on the performance of the array (see Garrett and Cummins [17]) and there are several ways to model it. Because this study is only concerned with the effects of the channel on the turbines via the global blockage, the issue of calculating seabed friction was

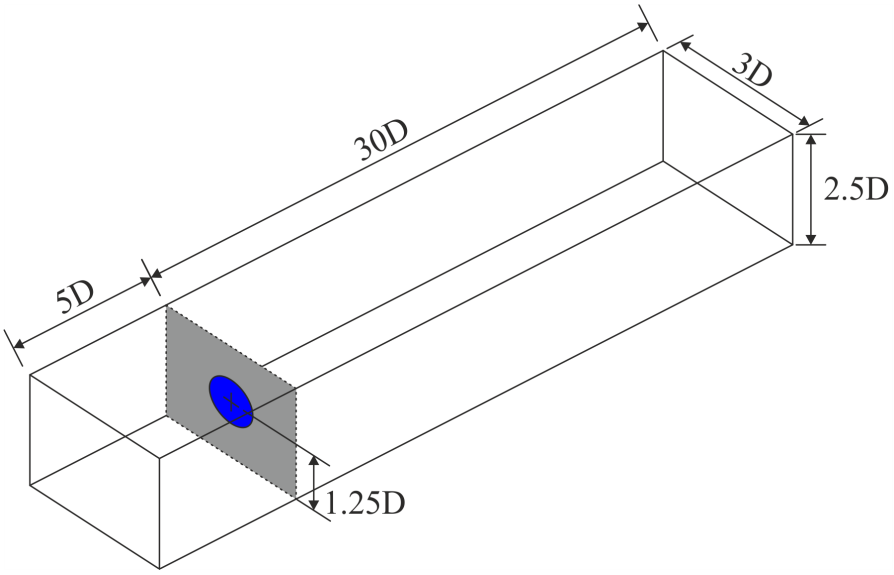

Figure 2.1: Computational domain for the single disc case (used for validation and normalising)

avoided by setting the seabed boundary condition to no-shear. Similarly, the effects of wind shear, waves and Langmuir turbulence from the sea surface were also neglected by setting the no shear boundary condition. Because all simulations used the same boundary conditions, the comparisons between simple disc and BEMT disc simulations are still valid. This approach was preferred for its simplicity and allowed a uniform inlet velocity profile to be used at the inlet boundary. The outlet condition was a zero-gradient outflow.

For the BEMT discs, it was not immediately obvious whether to set the nacelle wall boundary conditions to no-slip or no-shear. Several simulations were run with each option, and it was found that although there were some small differences in the near wake, the power coefficient calculation did not change by more than 2%, so a no-shear condition was used in all simulations, for simplicity.

The turbulence model used in the initial simulations was the $k-\omega$ SST model. The inlet turbulence was set by specifying a turbulence intensity of 10% and a hydraulic diameter based on the channel cross-sectional area and perimeter:

$$D_h = \frac{4.\text{Area}}{\text{Perimeter}}. \tag{2.1}$$

The validation simulations showed that changing the inlet turbulence intensity between 2% and 15% did not affect the results.

2.3 Source terms

The source terms inside the disc region were defined by introducing a user defined function (UDF), which is different for the two types of simulation.

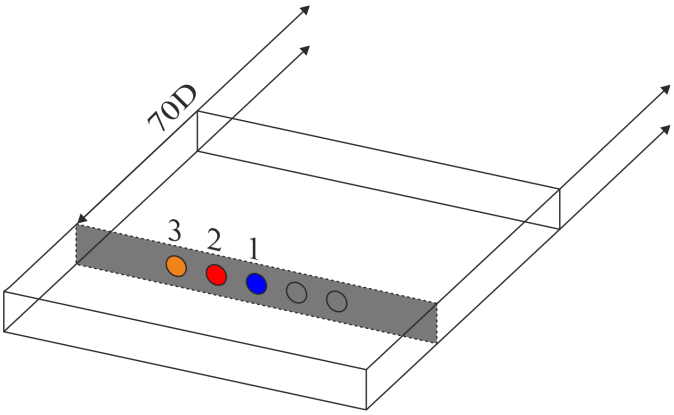

(a) Sketch of the computational domain for the whole array cases

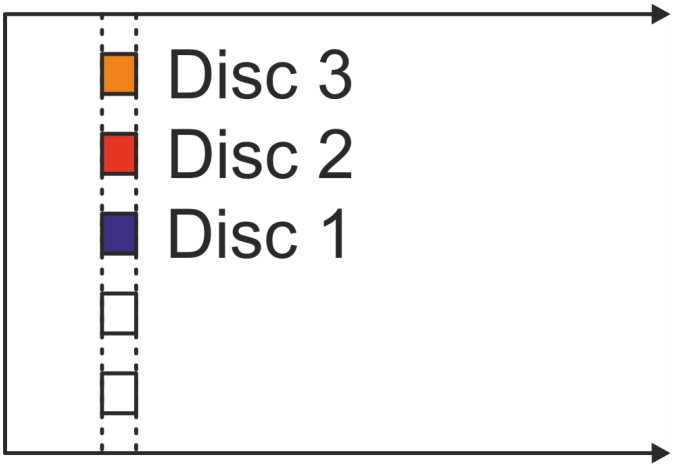

(b) Labelling of the discs in the whole array cases

Figure 2.2: Computational domain

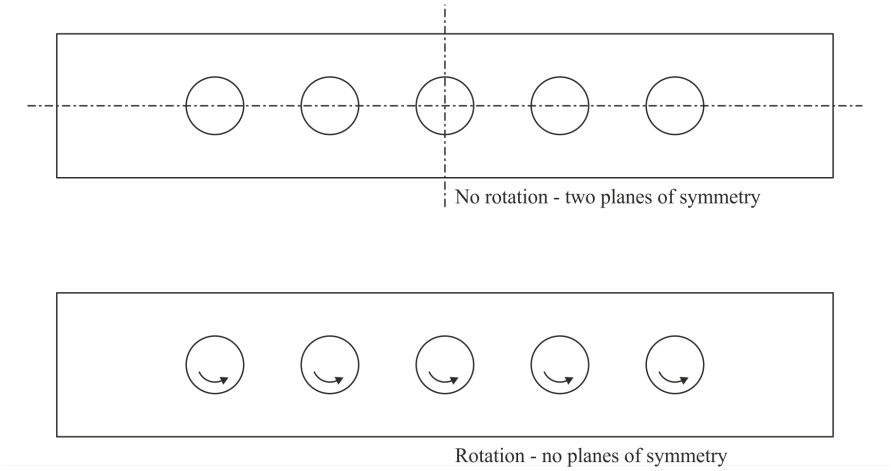

Figure 2.3: Comparison of the symmetry planes in front view between the simple disc full array case, and the BEMT disc full array case.

For the simple disc, a single UDF is sufficient to define a momentum sink in the x-direction. The UDF implements the source term

$$S_h = -\frac{K}{\Delta x}\frac{\rho}{2}U|U|, \tag{2.2}$$

where ρ is the fluid density, U is the local axial velocity, K is the extraction coefficient or momentum loss factor, and Δx accounts for the fact that the disc has a finite thickness in the computational mesh.

The source terms in a BEMT disc are more involved. First, lift and drag profiles are required for a given airfoil section. In this study, the section used is a standard NACA section with thickness and camber comparable to that of a typical tidal turbine, and the characteristics were obtained from Abbott and von Doenhoff [18]. The chord and twist angle characteristics used were those of a typical tidal turbine.

The lift and drag plots available from NACA only cover angles of attack from about -6° to 14°. Although the aerodynamic sections in a real tidal turbine will operate within this range, it is necessary to use appropriate values of C_L and C_D outside this range in order to guarantee convergence in CFD simulations. The approach of Batten *et al.* [19] was followed, whereby the lift coefficient was chosen to decay linearly from its maximum before stall (the stalled values of C_L were discarded since they could lead to divergence), and drag was set to increase linearly with incidence outside the defined data range. This approach gave good convergence and the angle of attack was always within the range covered by real data once the simulations had converged.

Finally, the source terms in the x, y and z directions are obtained by implementing the standard BEMT equations, as shown in Figure 2.4.

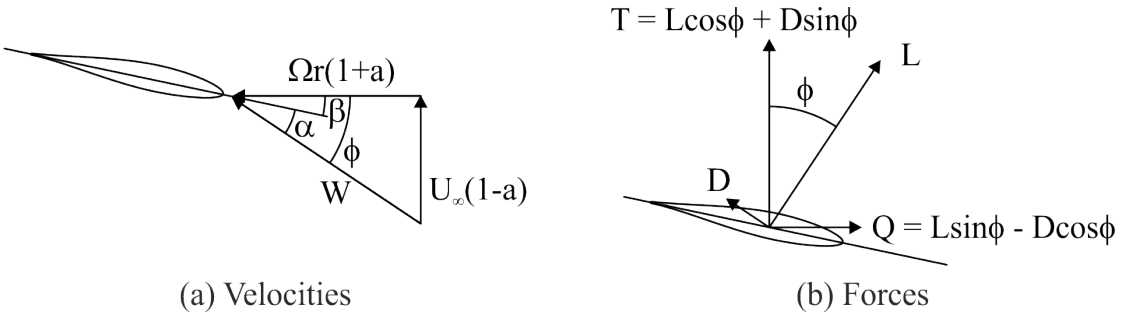

(a) Velocities (b) Forces

Figure 2.4: Velocities and forces in an airfoil section using Blade Element Momentum Theory. Figure reproduced from Ref. [18].

2.4 Post-processing

The main parameter of interest to the tidal farm designer is the power coefficient of the turbines, and it is therefore the main focus of this paper. In addition, axial velocity contours along the mid-plane (parallel to the seabed) are used for comparing flow fields qualitatively.

The power coefficient for simple discs is given by Equation 2.3, where $\langle u^3 \rangle$ is the cube of the axial velocity within the disc, averaged by cell volume:

$$C_P = K\frac{\langle u^3 \rangle}{U_\infty^3}. \tag{2.3}$$

For BEMT discs, the power coefficient is given in Equation 2.4 in terms of power P, which is equal to the angular velocity multiplied by the rotor torque, Q. The torque must therefore be calculated for BEMT discs by integrating Equation 2.5 along the cells inside the disc region.

$$C_P = \frac{P}{\frac{1}{2}\rho D U_\infty^3} = \frac{Q\Omega}{\frac{1}{2}\rho D U_\infty^3}, \tag{2.4}$$

$$Q = \int \frac{1}{2} W^2 B c(r) r \left(C_l \sin\phi - C_D \cos\phi\right) dr \tag{2.5}$$

3 Validation

3.1 Simple disc

The simple disc simulations were validated against Batten *et al.* [16] by simulating a single disc in a channel of the same dimensions. The results agreed both qualitatively and quantitatively and a comparison of the mid-plane velocity contours is given in Figure 3.1. The whole array case was validated against Nishino and Willden [8] through qualitative comparison of the velocity contours. Although in the latter case the channel geometries were not the same, the power coefficients obtained were in the same range.

In order to ensure a physically realistic dependence of power output on the momentum extraction coefficient K, a series of simulations were carried out in which K was varied systematically. This also enabled selection of an appropriate value of K for the simple disc array

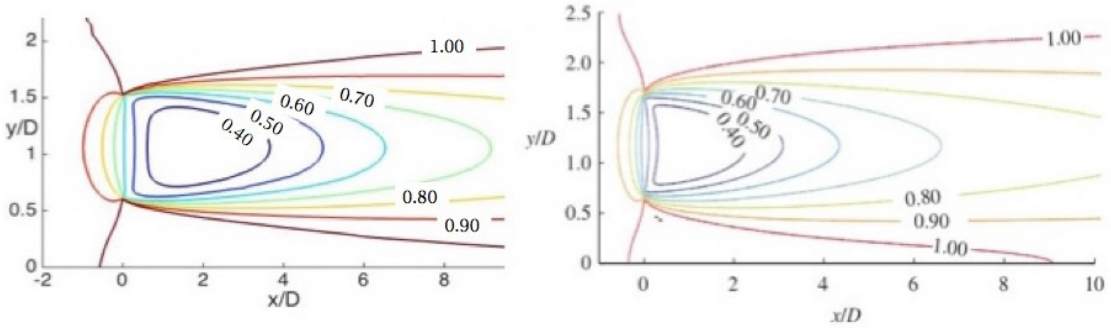

Figure 3.1: Validation of a simple disc simulation of a single turbine in a rectangular channel, showing normalised velocity contours along the mid-plane. Left: simulation. Right: Figure 10(b) reproduced from Batten *et al.* [16]

simulations. For these simulations, the global blockage was kept constant at 6.28%. Figure 3.2 shows the relationship between K and C_P from the simulations. Also shown in Figure 3.2 is the axial induction factor a of the turbine, which unlike K, is a physically meaningful parameter. As is to be expected, increasing K leads to an increase in a.

It can be seen from Figure 3.2 that when K is low, the turbine is under-exploiting the channel and the power output is low. The power output increases up to a maximum when K is approximately equal to 3. For high values of K, the high induction factor means that the turbine is greatly decelerating the incoming flow. In these cases, the disc is imposing too much resistance and so the flow is forced around the disc. The reduction in flow passing through the disc means that the power output decreases.

For a disc in an unconfined environment, the maximum power coefficient is given by the well known Betz limit of $C_P = 0.593$, and the corresponding induction factor can be shown analytically to be 1/3. A disc confined in a channel can reach a considerably higher power coefficient as shown in Figure 3.2. At a blockage of 6.28%, the maximum reached is $C_P = 0.685$ which occurs for a momentum loss factor of $K = 3$ with a corresponding induction factor of 0.39. This value of K was used for the full array simulations since it gives approximately maximum power output, and therefore in a real application the turbines would be designed to achieve a momentum extraction as close to this as possible.

Additionally, a set of runs were performed at different Reynolds numbers. The Reynolds number for this case is defined as,

$$Re = \frac{\rho U_{infty} D}{\mu}, \tag{3.1}$$

where D is the disc diameter. The simulations were performed on the same geometry, and the inlet velocity U_∞ was changed to give Reynolds numbers between 1.25×10^7 and 5×10^7. The variation in C_P was of the order of 1%. Therefore, the effect of the inlet velocity and Re was considered negligible for simulations at the scale considered here. The rest of the simulations were therefore run at a Reynolds number of 2.5×10^7.

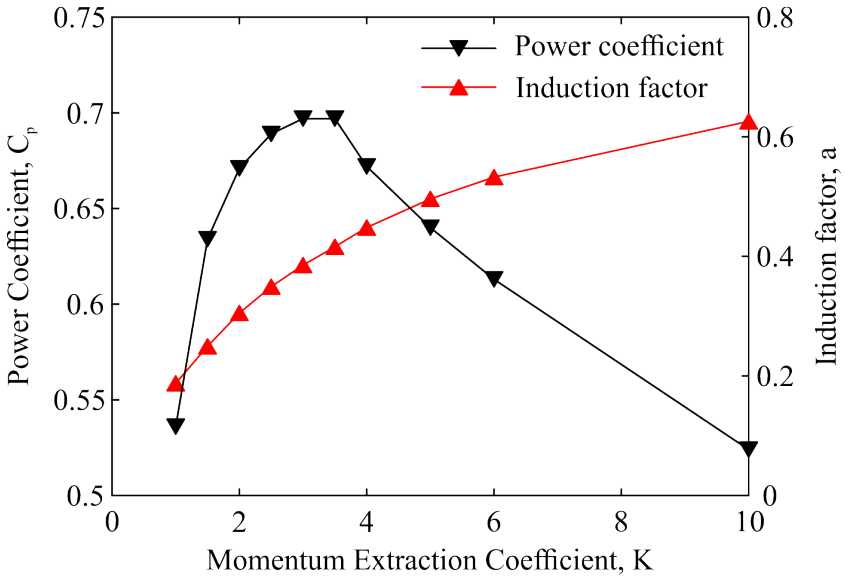

Figure 3.2: Power coefficient and induction factor of a single actuator disc against momentum loss factor K, for a constant blockage of $B_G = 6.28\%$

3.2 BEMT DISCS

When validating the BEMT simulations, no results in the literature were found against which to match simulations with the exact blade and channel geometry of this study. The approach followed was to run sets of simulations on a single disc in order to obtain a relationship between the simulation outputs and the input parameters. Because the input parameters in BEMT simulations have physical significance, the validity of those relationships can be verified. In the BEMT disc simulations, the parameters of interest are:

1. tip-speed-ratio, $TSR = \omega R/U$ (the ratio of the blade tip speed to the inlet flow speed),
2. lift and drag profiles,
3. Reynolds number.

The Reynolds number contribution had already been investigated using simple discs and there was no reason to believe that the BEMT discs would show a different dependence on it, so it was not investigated further. The dependence on different lift and drag profiles was not investigated either, since these are set by the turbine design. The tip speed ratio (TSR) is one of the main non-dimensional parameters of the operation of a real turbine. In a BEMT disc, it is the model parameter together with the lift and drag profiles and, unlike the momentum loss factor K in simple discs, it has physical significance.

A set of simulations was run to obtain a relationship between power coefficient and TSR for a single disc in a rectangular channel, holding the global blockage constant at 6.28%. The results are compared with the analytical relationship between C_P and TSR for an unconfined disc (such as a wind turbine), taken from Burton *et al.* [20]. The comparison is shown in Figure

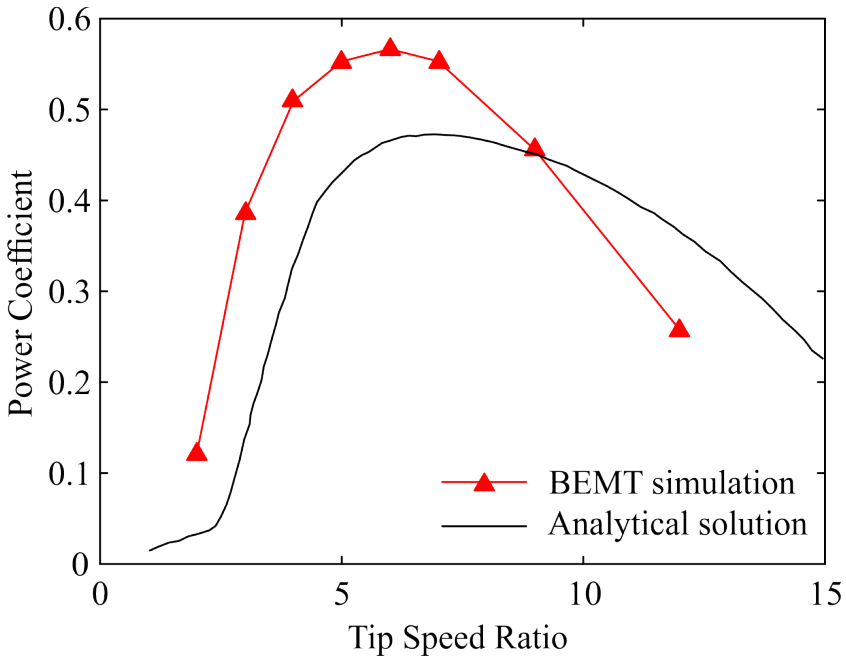

Figure 3.3: Validation of the method for BEMT disc simulations: power coefficient against tip-speed ratio (TSR). Continuous line: analytical relationship predicted for an unconned disc (such as a wind turbine), reproduced from Burton *et al.* [20]. Dashed line: simulations of a single BEMT disc in a rectangular channel with $B_G = 6.28\%$

3.3. As expected, the relationship between C_p and TSR is similar to the analytical one, with power output peaking at a TSR of about 6, but the values of power coefficient are higher than those for the unconfined case since power output is increased due to the effect of the channel blockage.

4 Results and Discussion

The main experiment in this study was the simulation of an array of 5 turbines in a rectangular channel. Two types of simulation were run: momentum-sink actuator discs (simple discs, with no swirl) and BEMT discs (with swirl). For each type of disc, a range of disc spacings between 0.25 and 3 diameters was simulated. Throughout all simulations, the Reynolds number (4.5×10^7), disc diameter (18 m) and disc thickness (0.18 m) were held constant.

For the simple disc simulations, the momentum loss factor K was kept constant as the spacing was varied. A value of $K = 3$ was used since this gave approximately maximum power for the single disc case in a channel of the same blockage (this is in contrast with the method used by Nishino and Willden [8] where K was adjusted to keep a constant global induction factor).

For the BEMT simulations, the lift and drag profiles used are those described in the Method section, and the discs were run at a constant TSR of 6. In addition, two cases were run with

BEMT discs at a lower TSR of 4.

4.1 Swirl effects: Qualitative comparison

Figure 4.1 shows three cases with the same geometry (spacing of 0.5 diameters and blockage of 6.28%) and provides a qualitative comparison of the effects of swirl. Figure 4.1(a) corresponds to BEMT discs at the optimal TSR of 6, Figure 4.1(b) corresponds to BEMT discs at a lower TSR of 4 (hence lower swirl), and Figure 4.1(c) corresponds to simple discs with no swirl.

By comparing the velocity contours, the effects of swirl on the interaction between discs become apparent. In the high swirl case (TSR 6) the wakes are highly distorted, with long dissipation lengths, large differences between discs (with the middle disc wake being the most distorted) and regions of flow recirculation with negative x-velocity. The simple disc case (with no swirl) conversely shows less distorted wakes which dissipate earlier and no recirculation, which implies that discs without swirl have less interaction at the same spacing. The low swirl case at TSR of 4 is clearly intermediate between the other two.

4.2 Quantitative comparison: power coefficient

Three sets of simulations were run of a five-disc array in a rectangular channel at different spacings: a set of simple disc simulations with $K = 3$ and high global blockage (6.28%), a set of BEMT discs at TSR of 6 and the same high blockage, and a further set of BEMT discs at the same TSR in a larger channel of the same aspect ratio but lower global blockage (0.5%). The results are given in Figure 4.2(a) for simple discs, high blockage; Figure 4.2(b) for BEMT discs, high blockage; and Figure 4.2(c) for BEMT discs, low blockage. The power coefficients are normalised by their value for a single disc of the same type in a channel of the same blockage, as shown in Table 4.1.

Table 4.1: Normalising power coefficients (single disc cases)

Type of disc	Channel blockage	Normalising C_p
Simple	6.28%	0.685
BEMT	6.28%	0.566
BEMT	0.50%	0.449

The simple disc results agree with published studies (Cooke *et al.* [21]). As the turbines get closer, the devices see an increase in their power output as they divert flow to each other, increasing the flow rate through the discs. This effect continues up to a spacing of 0.3 diameters, when the power output is maximised. If the discs are placed any closer, the diversion effect is saturated and the power coefficient starts to decrease again. Inspecting the velocity contours for a closely spaced case reveals that the whole array is now acting like a single disc, diverting flow away from the array (this case is comparable to a single actuator disc with too high a value of K, imposing too much resistance on the flow and hence operating sub-optimally).

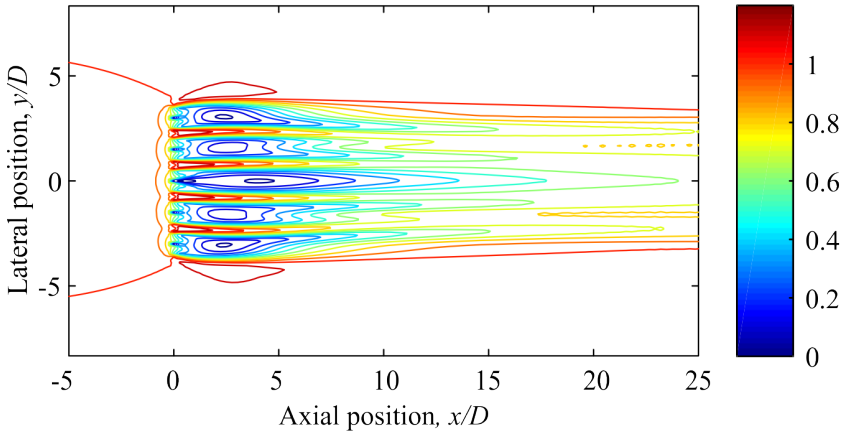

(a) BEMT discs, TSR = 6

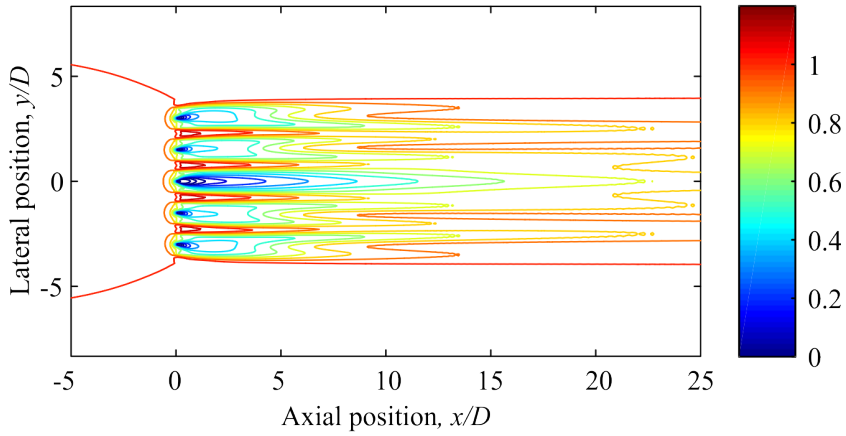

(b) BEMT discs, TSR = 4

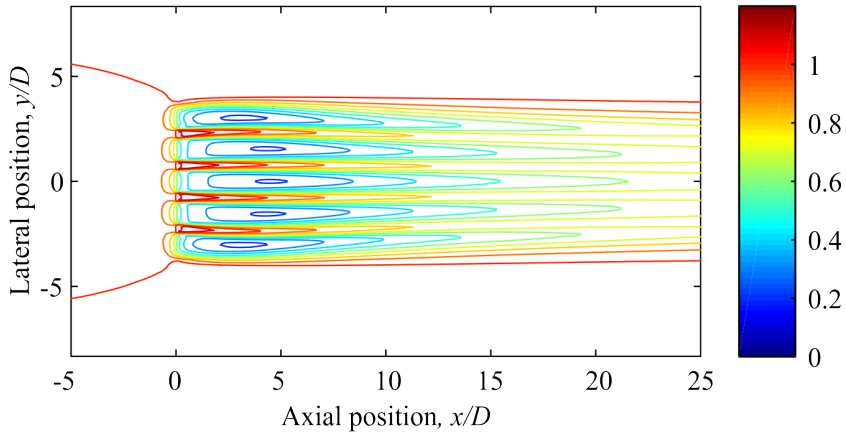

(c) Simple discs, K = 3.

Figure 4.1: Axial velocity contours for different types of disc in a 5-disc array with spacing $s = 0.5D$ and blockage $B_G = 6.28\%$

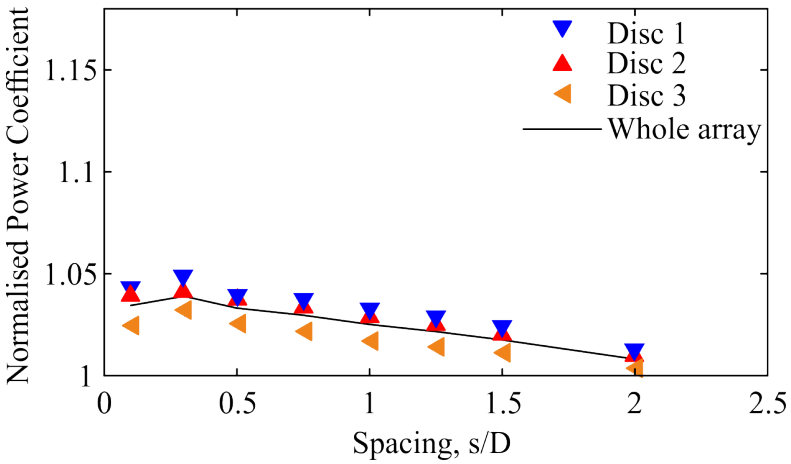

(a) Simple discs, K = 3, high blockage (Bg = 6.28%).

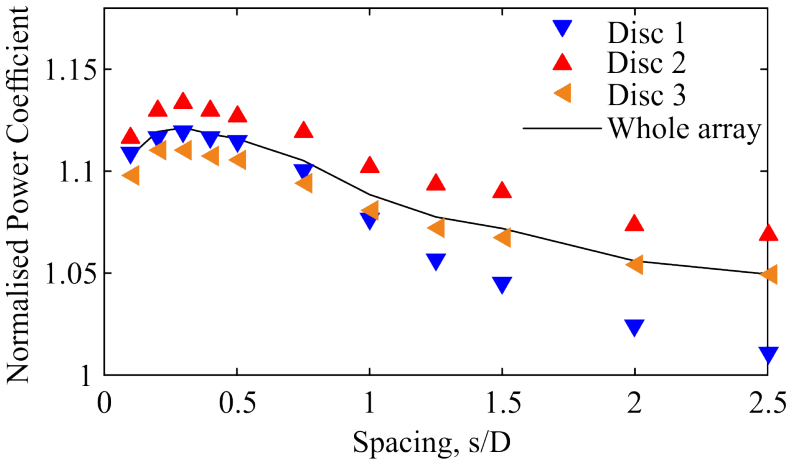

(b) BEMT discs, TSR = 6, high blockage (Bg = 6.28%).

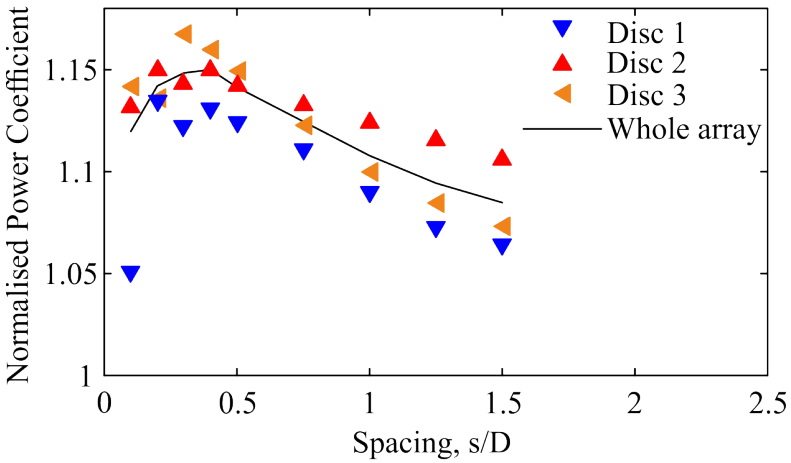

(c) BEMT discs, TSR = 6, low blockage (Bg = 0.5%).

Figure 4.2: Normalised power coefficient against turbine spacing with different disc configurations

In addition, since the power coefficient was calculated for each device separately, we can verify that the middle disc sees the greatest increase in performance, followed by the adjacent discs (disc 2), and the smallest increase is that of the edge discs (disc 3).

The BEMT results (Fig. 4.2(b) and (c), however, show a new effect that was not present before. In both the high and low global blockage cases, the turbines still see an increase in power output as the spacings get smaller, and experience a saturation effect for smaller spacings, with the maximum power being found at a spacing of approximately 0.3 diameters. However, when individual discs are compared, the greatest increase in performance no longer takes place at the middle disc. For most spacings and values of the blockage, the disc with the highest power output is the one labelled “Disc 2" rather than the middle disc.

The level of blockage is affects the results quantitatively as seen from the whole array results in Fig. 4.2 (b) and (c) (this would also be the case for simple discs). In addition, the results for the two blockage levels in panels (b) and (c) show a qualitative change, in that the power coefficients of the individual discs cross over at different levels of spacing. This suggests that the swirl-induced effects are channel-dependent, since they vary with global blockage.

5 CONCLUSIONS

Even with current high-performance computing power, full blade-geometry resolving high-fidelity numerical simulations, (either RANS or large-eddy simulations) of tidal turbine arrays remain too expensive to perform repeatedly over a large number of cases. The use of an actuator disc model greatly reduces the computational cost as individual blade boundary layers do not need to be resolved. In this paper, two different actuator disc models were considered: the simple actuator disc and the Blade Element Momentum Theory (BEMT) disc.

The simple disc model is the easiest to implement, but the momentum extraction coefficient K is not directly related to physical turbine parameters and must therefore be estimated. The use of BEMT discs removes this issue, as all the inputs are related to the real blade geometry and performance (C_L and C_D curves). The other key advantage of using BEMT discs is that they impart swirl onto the flow and thus provide a more realistic representation of the effect of the turbine on the flow. The increase in computational cost associated with implementing the BEMT disc is minimal. Other models where blade geometry is not resolved are actuator line model and actuator surface model, which also account for the transient effect of blade rotation. This study did not consider those simulations because the focus was on the steady-state effects of the swirl.

Comparisons between simulations with simple discs and BEMT discs showed that:

1. When the array is modelled with BEMT discs (with swirl), the flow field changes qualitatively from that produced by simple disc simulations, with highly distorted wakes, longer dissipation scales and flow recirculation in the near wake. This suggests that the swirl increases the interaction between turbines at a given spacing.

2. The peak power output was found at the same turbine spacing (0.3 diameters) in simulations with both types of discs. However, the value of peak power output was significantly

higher for the BEMT disc cases than the simple disc case. This suggests that the additional interaction between turbines due to swirl is advantageous for power output.

3. When the array is modelled with simple discs, the greatest increase in power is always found at the middle disc, regardless of turbine spacing. For closely-spaced arrays modelled with BEMT discs, however, the highest power coefficient is observed at intermediate discs. The reasons for this are unclear but it is believed to be due to the inclusion of swirl and the changes to the interaction between turbines that this introduces.

4. When the array is modelled using simple discs, the behaviour of the turbines is not channel-dependent. The proximity effects of BEMT disc arrays, however, change significantly with global blockage and hence are channel-dependent.

These four findings suggest that both the qualitative flow field and quantitative power output predictions generated by simple disc simulations will be inaccurate. It is therefore suggested that future studies should use actuator disc methods that include swirl, such as the BEMT discs used here or the actuator line and actuator surface models used in wind turbine literature. Because these methods do not resolve the blade geometry, the increase in computational cost is minimal while the additional insight into the flow is significant.

6 Acknowledgements

This technical note is published in memory of Rafa Baptista Ochoa, who undertook the simulations during and after his final year MEng project at the University of Cambridge and contributed to the writing prior to his death in 2017 (aged 23). The authors would also like to thank members of the Oxford Tidal Research Group for their help in the development of the work.

References

[1] R. Vennell. Exceeding the Betz limit with tidal turbines. *Renewable Energy*, 55:277–285, 2013.

[2] C. Garrett and P. Cummins. The power potential of tidal currents in channels. *Proc. R. Soc. A Math. Phys. Eng. Sci.*, 461(2060):2563–2572, 2005.

[3] A. Betz. Theoretical limit for best utilization of wind by wind-motors. *Magazine for the Entire Turbine System*, 26:307–309, 1920.

[4] I. G. Bryden and S. J. Couch. How much energy can be extracted from moving water with a free surface: A question of importance in the field of tidal current energy? *Renewable Energy*, 32(11):1961–1966, 2007.

[5] C. Garrett and P. Cummins. The efficiency of a turbine in a tidal channel. *Journal of Fluid Mechanics*, 588:243–251, 2007.

[6] R. Vennell. Tuning turbines in a tidal channel. *Journal of Fluid Mechanics*, 663:253–267, 2010.

[7] R. Vennell. Tuning tidal turbines in-concert to maximise farm efficiency. *Journal of Fluid Mechanics*, 671:587–604, 2011.

[8] Takafumi Nishino and Richard H.J. Willden. Two-scale dynamics of flow past a partial cross-stream array of tidal turbines. *Journal of Fluid Mechanics*, 730:220–244, 2013.

[9] Thomas A.A. Adcock, Scott Draper, Guy T. Houlsby, Alistair G.L. Borthwick, and Sena Serhadlioğlu. The available power from tidal stream turbines in the pentland firth. *Proceedings of the Royal Society A: Mathematical, Physical and Engineering Sciences*, 469(2157), 2013.

[10] Laith A.J. Zori and R. Ganesh Rajagopalan. Navier-Stokes calculations of rotor-airframe interaction in forward flight. *Journal of the American Helicopter Society*, 40(2):57–67, 1995.

[11] A. F. Molland and S. R. Turnock. A compact computational method for predicting forces on a rudder in a propeller slipstream. *Trans. Inst. Naval Archit.*, 138:227–244, 1996.

[12] R. F. Mikkelsen. *Actuator disc methods applied to wind turbines*. PhD thesis, Technical University of Denmark, 2003.

[13] A. MacLeod, S. Barnes, K. Rados, and I. G. Bryden. Wake effects in tidal current turbine farms. In *International Conference on Marine Renewable Energy*, pages 49–53, 2002.

[14] M. E. Harrison, W. M.J. Batten, and A. S. Bahaj. A blade element actuator disc approach applied to tidal stream turbines. *MTS/IEEE Seattle, OCEANS 2010*, 2010.

[15] W. M. J. Batten and A. S. Bahaj. CFD simulation of a small farm of horizontal axis marine current turbines. In A. A. M. Sayigh, editor, *World Renewable Energy Congress*, page 53455, Florence, Italy, 2006. Elsevier Science.

[16] W. M.J. Batten, M. E. Harrison, and A. S. Bahaj. Accuracy of the actuator disc-RANS approach for predicting the performance and wake of tidal turbines. *Philosophical Transactions of the Royal Society A: Mathematical, Physical and Engineering Sciences*, 371(1985), 2013.

[17] Chris Garrett and Patrick Cummins. Maximum power from a turbine farm in shallow water. pages 634–643, 2013.

[18] I. H. Abbott and A. E. von Doenhoff. *Theory of Wing Sections*. Dover Publications, Inc., New York, 1949.

[19] W. M.J. Batten, A. S. Bahaj, A. F. Molland, and J. R. Chaplin. The prediction of the hydrodynamic performance of marine current turbines. *Renewable Energy*, 33(5):1085–1096, 2008.

[20] T. Burton, D. Sharpe, N. Jenkins, and E. Bossanyi. *Wind Energy Handbook*. John Wiley & Sons, 2001.

[21] S. Cooke, R. H. J. Willden, and B. Byrne. Power and thrust behaviour in a porous disc fence array experiment. In *Oxford Tidal Energy Workshop*, 2015.